

The Effect of Large-Scale Transient Eddies on the Time-Mean Flow in the Atmosphere

EERO O. HOLOPAINEN AND L. RONTU

Department of Meteorology, University of Helsinki, Helsinki, Finland

NGAR-CHEUNG LAU

Geophysical Fluid Dynamics Program, Princeton University, Princeton, NJ 08540

(Manuscript received 3 February 1982, in final form 21 May 1982)

ABSTRACT

The effect of horizontal transports of momentum and heat by transient eddies (TE) on the time-mean flow is studied by examining the relevant terms in a local budget of quasi-geostrophic potential vorticity. Two long-term observational data sets are used, and results for the Northern Hemisphere winter are presented.

The results indicate that eddy heat fluxes in the free atmosphere exert a dissipative influence on both the zonally averaged flow and the stationary waves. On the other hand, eddy momentum transports tend to force cyclonic circulations over the semi-permanent Icelandic and Aleutian surface lows, and anticyclonic circulations over the oceanic high pressure cells in the subtropics. The forcing of the time-mean flow arising from horizontal TE heat transports is generally stronger than the forcing associated with eddy momentum transports. The net effect of eddy transports of heat and momentum is to dissipate the potential enstrophy of the stationary waves. The characteristic time scale associated with this dissipative effect is of the order of 4–5 days.

The relative contribution to the eddy forcing by low-frequency fluctuations (with periods between 10 days and a season) and by synoptic-scale fluctuations (with periods between 2.5 and 6 days) are examined. The forcing associated with low-frequency eddies generally dominates. The forcing associated with synoptic-scale eddies is concentrated in the cyclone tracks near the east coasts of Asia and North America, where a certain degree of counterbalancing between the heat flux forcing and the momentum flux forcing takes place.

1. Introduction

Observational data such as those compiled by Newell *et al.* (1974) indicate that about half of the kinetic energy in the atmosphere resides in the large-scale transient eddies¹ (TE), the other half being associated with the time-mean flow. The transports of heat and momentum by these transient motions have a dual effect on the stationary flow. The convergence of transient eddy flux of zonal momentum into the middle latitudes tends to accelerate the mean zonal flow, whereas the heat transports by these same eddies from warm to cold regions tend to smooth out the local temperature gradient, and thereby weaken the vertical shear of the time-mean flow. It is hence evident that the eddy transports of both momentum and heat must be taken into account in evaluating the net effect of the transient motions on the time-mean flow.

For zonally averaged flows, Edmon *et al.* (1980)

suggested that the net effect of TE may be studied using Eliassen-Palm (EP) cross sections. The divergence of the EP fluxes is the net zonal force exerted on the time-mean flow by the transient eddies. Edmon *et al.* pointed out that this force is approximately equal to the meridional transient eddy flux of quasi-geostrophic potential vorticity, and that it generally acts to decelerate the zonal mean flow in the free atmosphere. This result is consistent with the earlier finding reported by Wiin-Nielsen and Sela (1971), who showed that the observed eddy flux of quasi-geostrophic potential vorticity is equatorward in the troposphere above the boundary layer.

For atmospheric flows with variations in both the meridional and zonal directions, Saltzman (1962) studied the local effect of TE on the stationary waves by evaluating the contributions of the eddy transports of both heat and momentum to the time-mean budget of quasi-geostrophic potential vorticity. However, in most of the ensuing investigations, the local effect of eddy heat fluxes has been treated independently from that of eddy momentum fluxes (e.g., Holopainen, 1978; Lau, 1979; Holopainen and Oort, 1981a,b). These latter studies indicate that TE heat transports are directed down the local time-mean temperature

¹ As usual, "transient eddies" refer to motions which deviate from the seasonally averaged circulation, so that they include not only the time-varying zonal waves but also the transient component of the zonally averaged circulation.

gradient in the lower troposphere, and that momentum is redistributed by transient motions to counteract various local sources and sinks.

The present study aims at identifying the composite effects of the observed TE horizontal transports of heat and momentum on the zonally averaged as well as the local time-mean circulations. By doing so we hope to gain a proper perspective of the findings reported by the studies mentioned in the preceding paragraph. Only results for Northern Hemisphere winter are presented here. The data sets used for this investigation are described in Section 2. The eddy effects are considered within the framework of a quasi-geostrophic potential vorticity budget, which is formulated in Section 3. Results on the contribution of TE to this budget are presented in Section 4. The relative importance of eddy transports associated with low-frequency and synoptic-frequency fluctuations is discussed in Section 5.

2. Data sets

The following observational data sets are used in this study:

- **GFDL DATA.** These consist of monthly global objective analyses of circulation statistics accumulated at individual rawinsonde stations. The statistics for the 5-winter period from 1968-69 to 1972-73 used here are part of a larger 15-year set compiled by A. H. Oort at the Geophysical Fluid Dynamics Laboratory and have been used earlier (e.g., by Holopainen and Oort, 1981a,b). The winter season corresponds to the months of December, January and February.

- **NMC DATA.** These consist of circulation statistics based on twice-daily synoptic analyses produced by the U.S. National Meteorological Center. The domain of analysis extends from 20°N latitude to the North Pole. The statistics for a 8-winter period (1966-67 to 1968-69, 1970-71 to 1974-75) are used here. The winter season corresponds to the 120-day period beginning with 15 November. Further details of this data set have been documented by Lau *et al.* (1981). In the present study, the transient eddy statistics are first computed for each individual winter, and long-term averages of these seasonal statistics are then taken. Hence the transient eddies in a given winter refer to all fluctuations from the averaged circulation of that particular winter.

The GFDL and NMC data sets have been compared by Lau and Oort (1981, 1982).

3. Formulation of the potential vorticity budget

a. General considerations

Since the conservation of potential vorticity follows from the vorticity and thermodynamic energy equations, it is natural to study the composite effects

of TE transports of momentum and heat by examining the relevant terms in a potential vorticity budget.

Different forms of potential vorticity have been used in the literature. Many synoptic case studies (e.g., Staley, 1960) make use of one version of the original formulation by Ertel (1942), i.e.,

$$P_\theta = (\zeta_\theta + f)(-\partial\theta/\partial p).$$

Here ζ_θ is the relative vorticity defined on isentropic surfaces, f the Coriolis parameter, θ potential temperature and p pressure. It is evident from the definition of P_θ that the isentropic coordinate system would form the most natural framework for diagnosing the budget of this quantity. In several investigations on the planetary-scale general circulation (Hartmann, 1977; Savijärvi, 1978; Lau and Wallace, 1979), the relative vorticity defined on constant pressure surfaces (ζ_p) is used instead of ζ_θ , so that the analysis of the quantity

$$P_p = (\zeta_p + f)(-\partial\theta/\partial p)$$

may be performed in isobaric coordinates. In regions where P_θ and P_p exhibit strong vertical gradients, it is anticipated that transient and stationary vertical motions would play a significant role in the balances of these quantities. Moreover, budget studies of P_θ and P_p are complicated by the fact that the integrals of these quantities over an entire atmospheric column are infinite.

Several studies of potential vorticity (Wiin-Nielsen and Sela, 1971; Youngblut and Sasamori, 1980) have analyzed the quantity

$$Q = \zeta_p + f + \frac{\partial}{\partial p} \left(\frac{f_0^2}{\sigma} \frac{\partial\psi}{\partial p} \right), \tag{1a}$$

which, under quasi-geostrophic assumptions, is conserved following the nondivergent horizontal wind \mathbf{V}_ψ in isobaric coordinates (e.g., Holton, 1974), i.e.,

$$\left(\frac{\partial}{\partial t} + \mathbf{V}_\psi \cdot \nabla \right) Q = 0. \tag{1b}$$

Here ψ is the streamfunction, $\sigma = -(\alpha/\theta)\partial\theta/\partial p$ is a function of pressure only, α is the specific volume, and f_0 the Coriolis parameter at a reference latitude. Since the conservation law expressed in (1b) involves only horizontal motion on constant pressure surfaces, diagnosis of Q on the basis of conventional analyzed upper-air data is straightforward.

b. The quasi-geostrophic potential vorticity equation

In order to develop a framework for analyzing the observational data sets available at hand, we derive one form of the quasi-geostrophic potential vorticity equation in which the transient eddy transports of heat and momentum appear explicitly. The procedure followed here is analogous to that for the de-

riation of (1b). By starting with the primitive equations and retaining all terms in the intermediate steps, we also wish to gain a better appreciation of the assumptions involved in the quasi-geostrophic potential vorticity equation.

The time-averaged vorticity and thermodynamic energy equations may be written as

$$\frac{\partial \bar{\zeta}}{\partial t} = -\bar{\mathbf{V}} \cdot \nabla \bar{\eta} + \mathbf{k} \cdot \nabla \times \mathbf{A}_H + f \frac{\partial \bar{\omega}}{\partial p} + \mathbf{k} \cdot \nabla \times \bar{\mathbf{F}} + R_\zeta, \quad (2)$$

$$\mathbf{A}_H = \left(-\frac{1}{a \cos \phi} \frac{\partial}{\partial \lambda} \overline{u'u'} - \frac{1}{a \cos \phi} \frac{\partial}{\partial \phi} \overline{u'v'} \cos \phi + \frac{\overline{u'v'}}{a} \tan \phi \right) \mathbf{i} + \left(-\frac{1}{a \cos \phi} \frac{\partial}{\partial \lambda} \overline{u'v'} - \frac{1}{a \cos \phi} \frac{\partial}{\partial \phi} \overline{v'v'} \cos \phi - \frac{\overline{u'u'}}{a} \tan \phi \right) \mathbf{j} \quad (4)$$

is the horizontal acceleration of the time mean flow associated with the convergence of the horizontal transports of momentum by transient eddies; and

$$R_\zeta = \bar{\zeta} \frac{\partial \bar{\omega}}{\partial p} - \bar{\omega} \frac{\partial \bar{\zeta}}{\partial p} - \mathbf{k} \cdot \nabla \bar{\omega} \times \frac{\partial \bar{\mathbf{V}}}{\partial p} - \frac{\partial}{\partial p} (\mathbf{k} \cdot \nabla \times \overline{\mathbf{V}\omega'}).$$

As usual, a denotes the radius of the Earth, λ longitude, ϕ latitude, and $\mathbf{i}, \mathbf{j}, \mathbf{k}$ the unit vectors in the zonal, meridional and vertical direction, respectively.

Eq. (3) may be rewritten as

$$\bar{\omega} = \bar{S}^{-1} \left[\frac{\partial \bar{\theta}}{\partial t} + \bar{\mathbf{V}} \cdot \nabla \bar{\theta} + \nabla \cdot \overline{\mathbf{V}\theta'} + \frac{\partial}{\partial p} \overline{\omega'\theta'} - \frac{1}{c_p} \left(\frac{p_0}{p} \right)^{R/c_p} \bar{H} - \bar{S}'' \bar{\omega} \right]. \quad (5)$$

Here $S = -\partial\theta/\partial p$, the superscript tilde denotes hemispheric or global average and the double prime a deviation from this average. Substitution of (5) into (2) yields

$$\begin{aligned} \frac{\partial \bar{q}}{\partial t} + \bar{\mathbf{V}} \cdot \nabla \bar{q} &= f \underbrace{\frac{\partial}{\partial p} \left(\frac{\nabla \cdot \overline{\mathbf{V}\theta'}}{\bar{S}} \right)}_{A1} + \underbrace{\mathbf{k} \cdot \nabla \times \mathbf{A}_H}_{A2} + \underbrace{\mathbf{k} \cdot \nabla \times \bar{\mathbf{F}}}_{B} \\ &\quad - f \underbrace{\frac{\partial}{\partial p} \left[\frac{1}{c_p} \left(\frac{p_0}{p} \right)^{R/c_p} \bar{H} \bar{S}^{-1} \right]}_C + f \underbrace{\frac{\partial}{\partial p} \left[\bar{S}^{-1} \frac{\partial}{\partial p} (\omega'\theta') \right]}_D \\ &\quad - \underbrace{\frac{\partial}{\partial p} \left(\frac{\bar{S}'' \bar{\omega}}{\bar{S}} \right)}_E + f \bar{S}^{-1} \frac{\partial \bar{\mathbf{V}}}{\partial p} \cdot \nabla \bar{\theta} - \frac{\partial}{\partial p} \left(\frac{\bar{\theta}''}{\bar{S}} \right) \bar{\mathbf{V}} \cdot \nabla f \\ &\quad + f \frac{\partial}{\partial p} \left[\frac{\bar{\theta}}{\bar{S}^2} \frac{\partial \bar{S}}{\partial t} + \frac{\partial}{\partial t} \left(\frac{\bar{\theta}}{\bar{S}} \right) \right] + R_\zeta, \quad (6a) \end{aligned}$$

$$\frac{\partial \bar{\theta}}{\partial t} = -\bar{\mathbf{V}} \cdot \nabla \bar{\theta} - \bar{\omega} \frac{\partial \bar{\theta}}{\partial p} - \nabla \cdot \overline{\mathbf{V}\theta'} - \frac{\partial}{\partial p} \overline{\omega'\theta'} + \frac{1}{c_p} \left(\frac{p_0}{p} \right)^{R/c_p} \bar{H}. \quad (3)$$

Here the overbar denotes the time average, and the prime denotes deviation from time average; \mathbf{V} is the horizontal velocity vector; $\zeta = \mathbf{k} \cdot \nabla \times \mathbf{V}$, $\eta = \zeta + f$ the relative and absolute vorticity, respectively; ω is pressure velocity; \mathbf{F} is friction associated with subgrid-scale processes; c_p the specific heat at constant pressure; R the gas constant; $p_0 = 1000$ mb; H the diabatic heating per unit mass;

where

$$\bar{q} = \bar{\zeta} + f - f \frac{\partial}{\partial p} \left(\frac{\bar{\theta}''}{\bar{S}} \right) \quad (6b)$$

is one form of potential vorticity similar to that defined in Eq. (1a).

For quasi-geostrophic motion and for uniform f , those terms in (6a) involving R_ζ , $\partial \bar{\mathbf{V}}/\partial p \cdot \nabla \bar{\theta}$, $\bar{\mathbf{V}} \cdot \nabla f$ and the time variation of the average static stability may be neglected. The principal sources and sinks in the budget of \bar{q} are then seen to be associated with

- Horizontal TE transports of heat (term A1) and momentum (term A2). We shall be concerned exclusively with these effects in the present study.
- Curl of frictional forces related to subgrid-scale processes (term B).
- Vertical gradient of the diabatic heating field (term C).
- Vertical heat transports by transient eddies (term D). Some evidence (e.g., Schubert and Herman, 1981) suggests that this effect may be important, especially in baroclinically active regions.
- Horizontal variation of \bar{S} (term E). The results presented by Tomatsu (1979) indicate that the static stability parameter for different geographical locations vary by a factor of 2-3 in the wintertime troposphere. Results based on the assumption of constant static stability may hence be subject to considerable uncertainties.

c. Transient eddy forcing

We first define the terms A1 and A2 in (6a) as

$$D^{\text{HEAT}} = f \frac{\partial}{\partial p} \left(\frac{\nabla \cdot \overline{\mathbf{V}\theta'}}{\bar{S}} \right), \quad (7a)$$

$$D^{\text{VORT}} \equiv \mathbf{k} \cdot \nabla \times \mathbf{A}_H = -\nabla \cdot \overline{\mathbf{V}'\zeta'}, \quad (7b)$$

with the second equality in (7b) being valid for horizontally non-divergent flows. The most immediate contribution of TE fluxes to the potential vorticity budget may be qualitatively described as follows: vertical variations of the convergence of TE heat transports (7a) influence the local static stability and thereby lead to changes in the third term in (6b), whereas eddy momentum transports in (7b) affect the vorticity of the time mean flow [i.e., the first term in (6b)]. Additionally, the TE fluxes also exert less direct influences on the mean flow through their association with induced circulations.

By assuming that f is constant, the eddy effects represented in (7a) and (7b) may be related to the convergence of TE potential vorticity transport, i.e.,

$$D = D^{\text{HEAT}} + D^{\text{VORT}} = -\nabla \cdot \overline{\mathbf{V}'q'}. \quad (8)$$

In order to aid the interpretation of results (see also Holopainen, 1982), it is useful to visualize that the transient eddies act on the time mean flow through the non-divergent "forces" $\mathbf{F}_\psi^{\text{HEAT}}$, $\mathbf{F}_\psi^{\text{VORT}}$ which are defined as

$$D^{\text{HEAT}} = \mathbf{k} \cdot \nabla \times \mathbf{F}_\psi^{\text{HEAT}} = \nabla^2 \psi^{\text{HEAT}}, \quad (9a)$$

$$D^{\text{VORT}} = \mathbf{k} \cdot \nabla \times \mathbf{F}_\psi^{\text{VORT}} = \nabla^2 \psi^{\text{VORT}}. \quad (9b)$$

Here ψ^{HEAT} and ψ^{VORT} are streamfunctions related to the nondivergent forces by

$$\left. \begin{aligned} \mathbf{F}_\psi^{\text{HEAT}} &= \mathbf{k} \times \nabla \psi^{\text{HEAT}} \\ \mathbf{F}_\psi^{\text{VORT}} &= \mathbf{k} \times \nabla \psi^{\text{VORT}} \end{aligned} \right\}.$$

The definitions in (9) are motivated by the following considerations. Inspection of the expressions for D^{VORT} and \mathbf{A}_H in (7b) and (4), respectively, reveals that $\mathbf{F}_\psi^{\text{VORT}}$ as defined in (9b) is equal to \mathbf{A}_H , where the subscript ψ denotes the nondivergent component. Hence $\mathbf{F}_\psi^{\text{VORT}}$ may be interpreted as the acceleration of the nondivergent component of the time-mean flow resulting from the convergence of horizontal momentum transports by transient eddies. The physical interpretation of $\mathbf{F}_\psi^{\text{HEAT}}$ as defined in (9a) is not as straightforward as that of $\mathbf{F}_\psi^{\text{VORT}}$. However, by devising a relationship between $\mathbf{F}_\psi^{\text{HEAT}}$ and D^{HEAT} [Eq. (9a)] which is analogous to that between $\mathbf{F}_\psi^{\text{VORT}}$ and D^{VORT} [Eq. (9b)], we anticipate that the patterns of $\mathbf{F}_\psi^{\text{HEAT}}$ and $\mathbf{F}_\psi^{\text{VORT}}$ obtained therefrom should serve as instructive diagnostic aids for examining the individual roles of heat transports and momentum transports by the transient eddies in forcing the nondivergent component of the time-mean flow. It is worth noting that the irrotational parts of the forces, even if possibly of the same order of magnitude as the nondivergent parts, are of no real importance because they only enter into the mean divergence equation, where their contributions are relatively much smaller than the contributions associated

with the pressure gradient force and the Coriolis force.

4. Forcing by transient eddies of all time scales

The results presented in this section are based on circulation statistics for unfiltered time series, so that the transient eddies to be described here represent fluctuations with time scales ranging from a day to a season. Except for part of Fig. 5, all results in this section pertain to the GFDL data set for Northern Hemisphere winter.

a. Zonally-averaged forcing

Fig. 1 shows the latitude-height distribution of the zonally averaged values of D^{HEAT} , D^{VORT} and D . The pattern for D^{HEAT} may be understood in light of the temperature tendencies associated with eddy heat transports. The poleward eddy heat flux across the mid-latitudes acts to cool the subtropics and warm the higher latitudes. Such temperature tendencies are strongest in the lower troposphere, where the most intense heat transfer occurs (Oort and Rasmusson, 1971; Lau *et al.*, 1981). This configuration of warming and cooling tends to stabilize the middle troposphere equatorward of about 50°N and 50°S, and destabilize the atmosphere poleward of these latitudes. In the Northern Hemisphere, stabilization is associated with positive tendency of \bar{q} , and *vice versa* [see Eq. (6b)]. The reverse situation applies to the Southern Hemisphere, where f is negative.

Similarly, the features for D^{VORT} may be related to the zonal wind tendencies associated with eddy momentum transports. The predominantly poleward momentum fluxes in the subtropics and equatorward fluxes in the higher latitudes (Oort and Rasmusson, 1971; Lau *et al.*, 1981) tend to accelerate the zonal wind between 35° and 55° in both hemispheres, and to decelerate the zonal wind both poleward and equatorward of these latitude belts. In the Northern Hemisphere, these zonal wind changes would be accompanied by positive vorticity tendency between 40 and 60°N, and negative vorticity tendency in the subtropics. The sign of these tendencies is reversed in the Southern Hemisphere.

Comparison between D^{HEAT} and D^{VORT} reveals that the magnitude of D^{HEAT} is generally larger than that of D^{VORT} , particularly in the higher latitudes. At a given latitude, the sign of D^{VORT} is fairly uniform with height, whereas the sign of D^{HEAT} exhibits much more variations in the vertical direction. There exists a certain degree of cancellation between D^{HEAT} and D^{VORT} in the middle latitudes, where the forcing of the zonal wind associated with the convergence of eddy momentum transports is partially offset by diminished meridional thermal gradient and vertical wind shear resulting from the eddy heat fluxes. The magnitudes of D^{HEAT} and D^{VORT} over the tropics are generally small. This finding needs to be interpreted

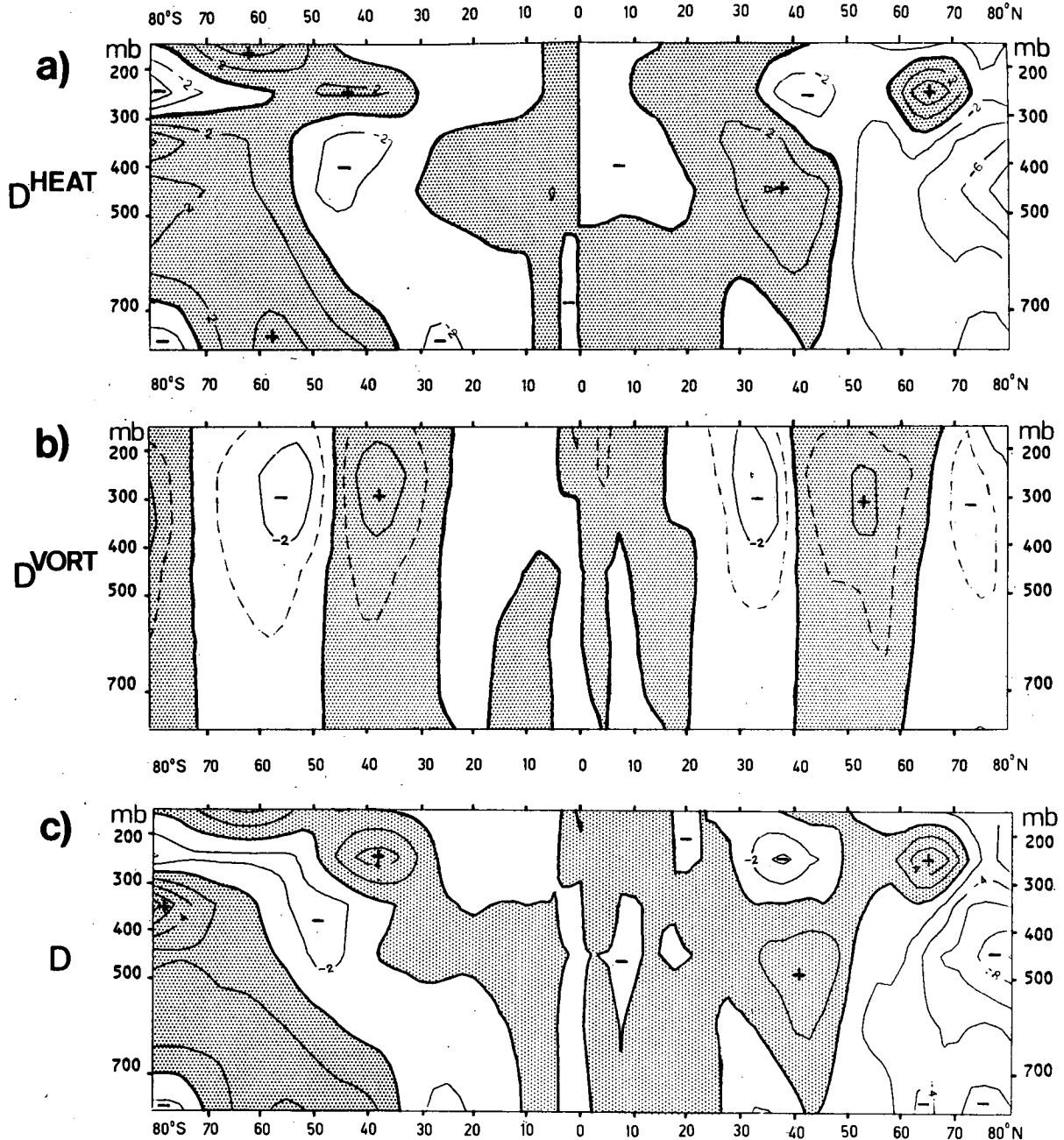


FIG. 1. Latitude-height distribution of the zonally averaged values of (a) D^{HEAT} , (b) D^{VORT} and (c) $D (=D^{\text{HEAT}} + D^{\text{VORT}})$ for December-February, as determined from GFDL data. Units: 10^{-11} s^{-2} .

in the context of the quasi-geostrophic formulation of the budget for \bar{q} [Eq. (6)]. However, we note here that no geostrophic approximation has been made in the computation of the terms D^{HEAT} and D^{VORT} themselves, since actual observed wind data have been used in compiling the pertinent eddy statistics at all latitudes.

The zonally averaged distributions of the zonal components of F_{ψ}^{HEAT} , F_{ψ}^{VORT} and $F_{\psi}^{\text{HEAT}} + F_{\psi}^{\text{VORT}}$ are shown in Fig. 2. The zonal force associated with the horizontal TE heat fluxes (F_{ψ}^{HEAT}) is negative almost

everywhere in the free troposphere. This force is strongest in the middle troposphere between 50 and 60°N, where it attains a magnitude of almost $10 \times 10^{-5} \text{ m s}^{-2}$. The pattern of the zonal force associated with TE momentum fluxes (F_{ψ}^{VORT}) is consistent with the preceding discussion pertaining to D^{VORT} . The magnitude of F_{ψ}^{VORT} is generally smaller than that of F_{ψ}^{HEAT} , as can be expected from the dominance of D^{HEAT} over D^{VORT} (Fig. 1).

After taking into account the different definitions used, the distribution of the total zonal force (Fig.

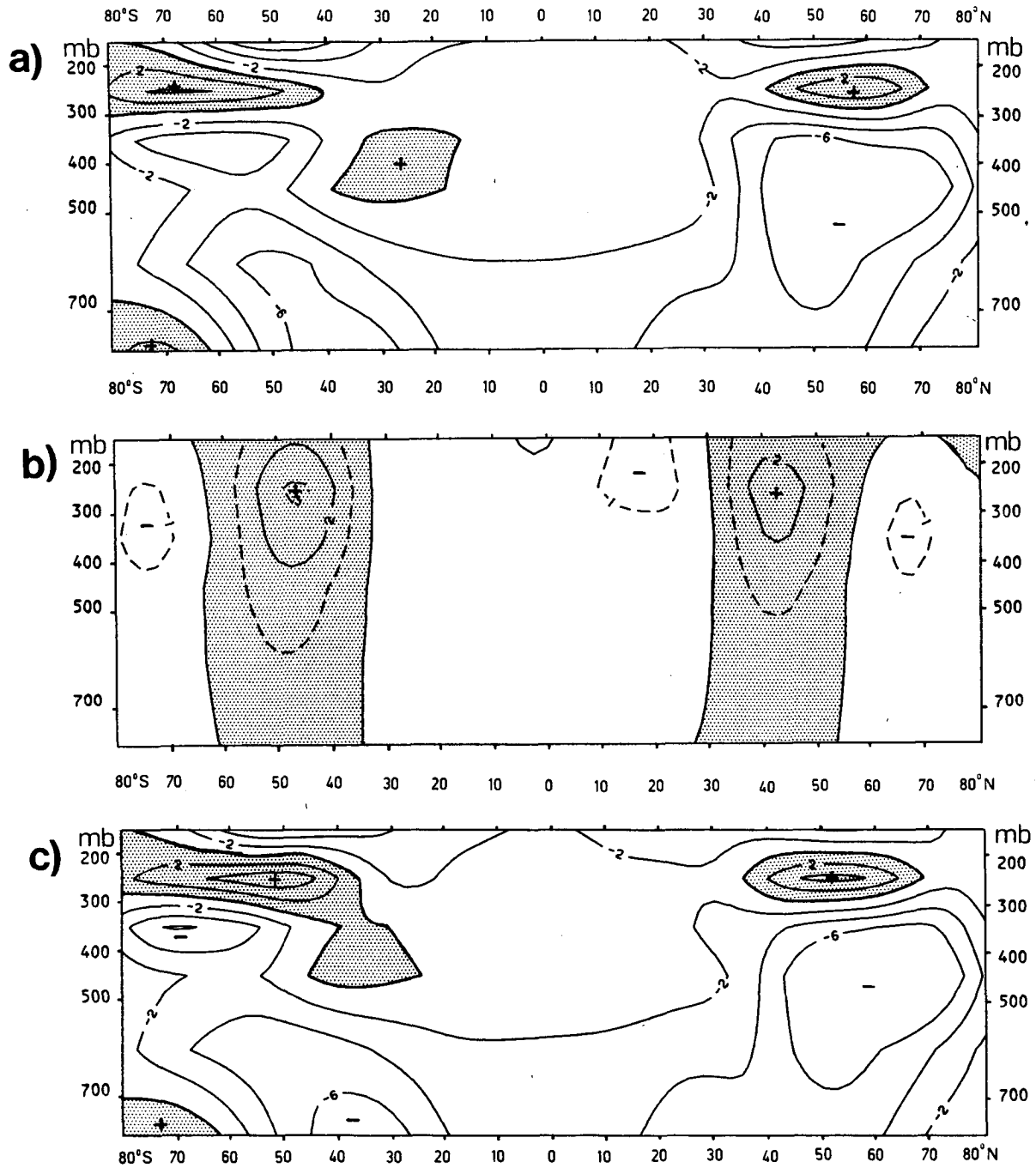


FIG. 2. Latitude-height distribution of the zonally averaged values of the zonal component of (a) F_{ψ}^{HEAT} , (b) F_{ψ}^{VORT} and (c) $F_{\psi}^{\text{HEAT}} + F_{\psi}^{\text{VORT}}$ for December-February, as determined from GFDL data. Units: $10^{-5} \text{ m}^2 \text{ s}^{-2}$.

2c) is seen to be in good agreement with that computed by Edmon *et al.* (1980, Fig. 1) on the basis of Eliassen-Palm flux divergence.

b. Geographical distribution of transient eddy forcing

In this subsection, the local variation of transient eddy forcing is examined by mapping the quantities

D^{HEAT} and D^{VORT} , as well as the corresponding streamfunctions ψ^{HEAT} and ψ^{VORT} . The streamfunctions are computed by expanding D^{HEAT} , D^{VORT} , ψ^{HEAT} and ψ^{VORT} in terms of spherical harmonics Y_m^n , and then solving for the coefficients of ψ^{HEAT} , ψ^{VORT} using the definitions in (9). Here n is the total wavenumber and m the zonal wavenumber. The results presented in Figs. 3 and 4 are obtained by retaining coefficients for $m \leq 10$ and $n \leq 20$.

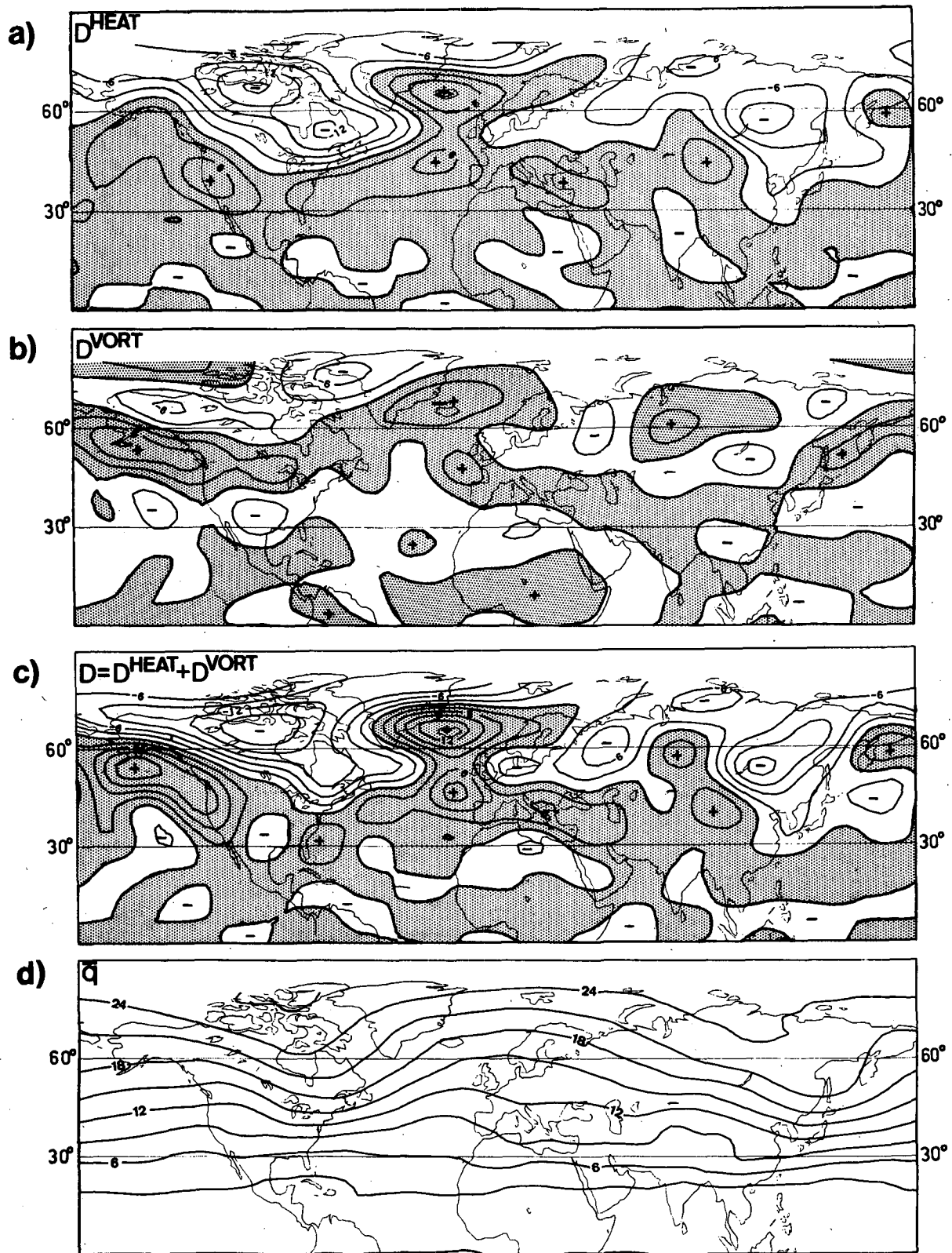


FIG. 3. Hemispheric wintertime distribution of (a) D^{HEAT} , (b) D^{VORT} and (c) $D (=D^{\text{HEAT}} + D^{\text{VORT}})$ —units: 10^{-11} s^{-2} —and (d) \bar{q} —units: 10^{-5} s^{-1} —for December–February in the layer 300–700 mb, as determined from the GFDL data.

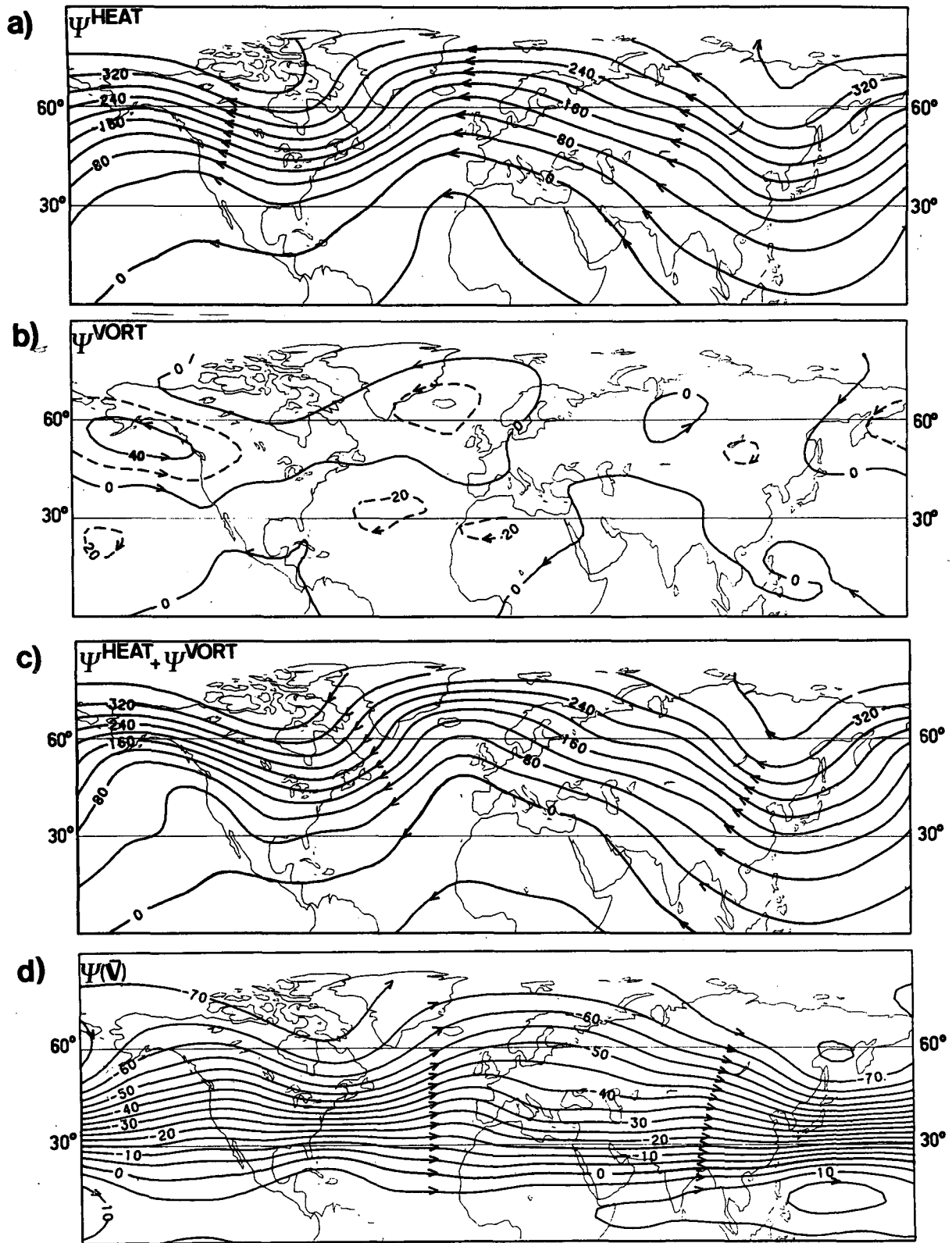


FIG. 4. Hemispheric wintertime distribution of (a) ψ^{HEAT} , (b) ψ^{VORT} and (c) $\psi^{\text{HEAT}} + \psi^{\text{VORT}}$ (units: $\text{m}^2 \text{s}^{-2}$) and (d) streamfunction of the time-mean flow (units: $10^6 \text{m}^2 \text{s}^{-1}$), for December-February in the layer 300-700 mb, as determined from the GFDL data. The direction of the forces F_{ψ}^{HEAT} , F_{ψ}^{VORT} and $F_{\psi}^{\text{HEAT}} + F_{\psi}^{\text{VORT}}$ is indicated by arrow heads in (a)-(c).

The patterns of D^{HEAT} and D^{VORT} averaged over the atmospheric layer between 700 and 300 mb are shown in Figs. 3a and 3b, respectively. It is seen that the two patterns are positively correlated over several regions, so that the sum (shown in Fig. 3c) attains large amplitude over these same locations. Notable examples are the positive values over Iceland and off the western shores of North America, and the negative values over northern Canada.

Comparison of the patterns for D (Fig. 3c) and \bar{q} (Fig. 3d) reveals that the departures from zonal average of those two quantities tend to be negatively correlated. Since D is related to the convergence of TE transport of potential vorticity [Eq. (8)] this result implies that the transient motions act to suppress the deviation from zonal symmetry of \bar{q} by redistributing potential vorticity. This dissipative effect will be further examined in Section 4c in the context of the potential enstrophy budget.

The distributions of the streamfunctions ψ^{HEAT} and ψ^{VORT} are shown in Figs. 4a and 4b, respectively. The direction of the forces F_{ψ}^{HEAT} and F_{ψ}^{VORT} associated with these streamfunctions is indicated by arrowheads. F_{ψ}^{HEAT} has an easterly component almost everywhere. Its wavelike pattern (Fig. 4a) is dominated by anticyclonic curvature over eastern Asia and eastern North America, and cyclonic curvature over the northeastern portion of the two ocean basins. F_{ψ}^{HEAT} attains its maximum amplitude of about $12 \times 10^{-5} \text{ m s}^{-2}$ over Alaska.

The most prominent features in the pattern for F_{ψ}^{VORT} (Fig. 4b) are the closed cyclonic cells over Iceland and the Gulf of Alaska, and the anticyclonic cells over the subtropical oceans. Between the pairs of cyclonic and anticyclonic cells is a zonal belt where F_{ψ}^{VORT} is directed eastward, with a magnitude of about $3 \times 10^{-5} \text{ m s}^{-2}$. Since the magnitude of F_{ψ}^{HEAT} is generally larger than that of F_{ψ}^{VORT} , the pattern for $\psi^{\text{HEAT}} + \psi^{\text{VORT}}$ (shown in Fig. 4c) is dominated by the features in ψ^{HEAT} .

Comparison of the patterns for $\psi^{\text{HEAT}} + \psi^{\text{VORT}}$ (Fig. 4c) and the observed wintertime streamfunction of the time mean flow (Fig. 4d) indicates that $F_{\psi}^{\text{HEAT}} + F_{\psi}^{\text{VORT}}$ tends to oppose the time-averaged circulation almost everywhere. Hence TE transports of heat and momentum not only act to decelerate the zonally averaged flow (as was demonstrated in Fig. 2c), but also exert a damping effect on the stationary waves. The latter finding is in conformity with the discussion pertaining to Figs. 3c and 3d.

c. Effect of transient eddies on the potential enstrophy of stationary waves

One measure of the intensity of the stationary waves is the potential enstrophy

$$B = \frac{1}{2}[\bar{q}^*{}^2],$$

where the bracket denotes zonal average and the asterisk a deviation from zonal average. As can be shown through manipulation of Eqs. (6) and (8), the TE transports enter the potential enstrophy budget of the stationary waves through the covariance quantity $[D^* \bar{q}^*]$.

In Fig. 5 is shown the latitude-height distributions of B and $[D\bar{q}^*]$ for Northern Hemisphere winter, as computed using the GFDL and NMC data sets. The pattern for B (upper panels of Fig. 5) is characterized by a primary maximum in the upper troposphere. The numerical values of potential enstrophy are seen to be an order of magnitude larger than those of enstrophy $\{\frac{1}{2}[\bar{q}^*{}^2]\}$ reported by Holopainen and Oort (1981b). It is hence evident that by far the most significant contribution to B comes from the term $-f\partial(\bar{\theta}^* \bar{S}^{-1})/\partial p$ [see (6b)].

The quantity $[D^* \bar{q}^*]$ is negative almost everywhere (Fig. 5, bottom panel). This is largely a reflection of the negative spatial correlation between D^{HEAT} and \bar{q} (Figs. 3a and 3d). Since we have concluded in the preceding paragraph that the largest contribution to \bar{q} comes from the term $-f\partial(\bar{\theta}^* \bar{S}^{-1})/\partial p$, the role of the transient eddies in the balance of B is seen to be essentially determined by the local influences of the eddy heat transports on the time-averaged static stability. In the present context, the effects of D^{VORT} on the enstrophy $\{\frac{1}{2}[\bar{q}^*{}^2]\}$, as examined by Holopainen and Oort (1981b), appear to play a less important role. A measure of the time scale associated with the dissipative effects of the transient eddies on B is the quantity $B/[D^* \bar{q}^*]$. Upon substitution of values representative of the extratropics, this time scale is estimated to be approximately 4–5 days. This result agrees with that reported by Lau (1979) considering only eddy heat fluxes, and by Youngblut and Sasamori (1980) considering eddy potential vorticity fluxes.

Although the two observational data sets yield qualitatively similar results, noticeable differences exist between the GFDL and NMC patterns for $[D^* \bar{q}^*]$ (bottom panels of Fig. 5). Such discrepancies are probably related to the deviations between the two data compilations over the data-sparse regions, as have been documented by Lau and Oort (1981, 1982).

5. Forcing by synoptic-scale and low-frequency fluctuations

In Fig. 6 is shown the distribution of the streamfunctions ψ^{HEAT} and ψ^{VORT} , as computed using time-filtered NMC data² averaged over the atmospheric layer between 700 and 300 mb. The low-pass and

² The computer subroutine PWSSSP described in NCAR (1978) is used to solve (9) for ψ^{HEAT} and ψ^{VORT} with the boundary conditions that $\psi^{\text{HEAT}} = 0$ and $\psi^{\text{VORT}} = 0$ at 20°N.

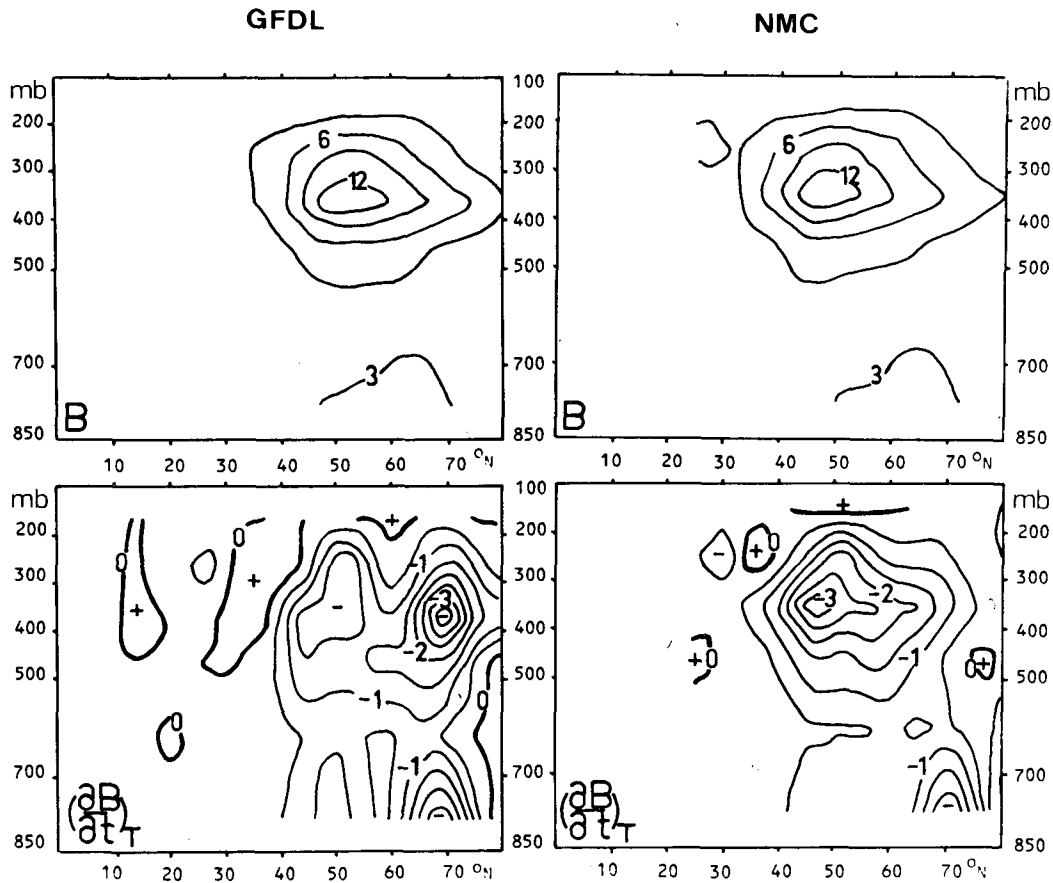


FIG. 5. Latitude-height distribution of $B = \frac{1}{2}[\bar{q}^{*2}]$, upper panels (units: 10^{-10} s^{-2}) and $(\partial B / \partial t)_T = [D^* \bar{q}^*]$, lower panels (units: 10^{-15} s^{-3}), for winter, as determined from GFDL data (left) and NMC data (right).

band-pass filters used here retain fluctuations with periods of 10 days to a season and 2.5–6 days, respectively [refer to Blackmon (1976) for further details].

Inspection of Figs. 4 and 6 reveals that the heat and vorticity transports by low-frequency disturbances account for a large fraction of the total eddy forcing. For example, the cyclonic cells noted in ψ^{VORT} over the Gulf of Alaska and Iceland (Fig. 4b, based on unfiltered data) are seen to be almost entirely associated with vorticity transports by long-period disturbances (Fig. 6, upper right panel). For both low-pass and band-pass fluctuations, the eddy effect due to heat transports is stronger than that due to vorticity transports. The forcing associated with vorticity and heat transports by low-frequency fluctuations tend to cooperate with each other over the northeastern portion of the Pacific and Atlantic, where both ψ^{HEAT} and ψ^{VORT} based on low-pass filtered data (Fig. 6, upper panels) exhibit a distinct cyclonic curvature. On the other hand, the accelerations accompanying the heat and vorticity transports by band-pass fluctuations tend to oppose each other between 35 and 50°N at most longitudes (Fig.

6, lower panels). The strongest cancellation between F_{ψ}^{HEAT} and F_{ψ}^{VORT} based on band-pass filtered data occurs off the eastern seaboard of Asia and North America. These regions are coincident with the wintertime cyclone tracks, where the band-pass eddy statistics are characterized by strong poleward heat transports as well as strong convergence of momentum transports (Blackmon *et al.*, 1977).

6. Discussion

The present observational study of the effect of large-scale transient eddies on the time-mean flow in the atmosphere complements earlier studies on this subject in the sense that more extensive data sets are used, that the composite effects of eddy fluxes of heat and momentum are emphasized throughout, and that the long-period and synoptic-scale fluctuations are treated separately.

The results show that the large-scale transient eddies have a strong dissipative effect on the time-mean flow. This result, obtained here in the framework of potential vorticity, is compatible with the results on the observed energy cycle presented by Lau and Oort

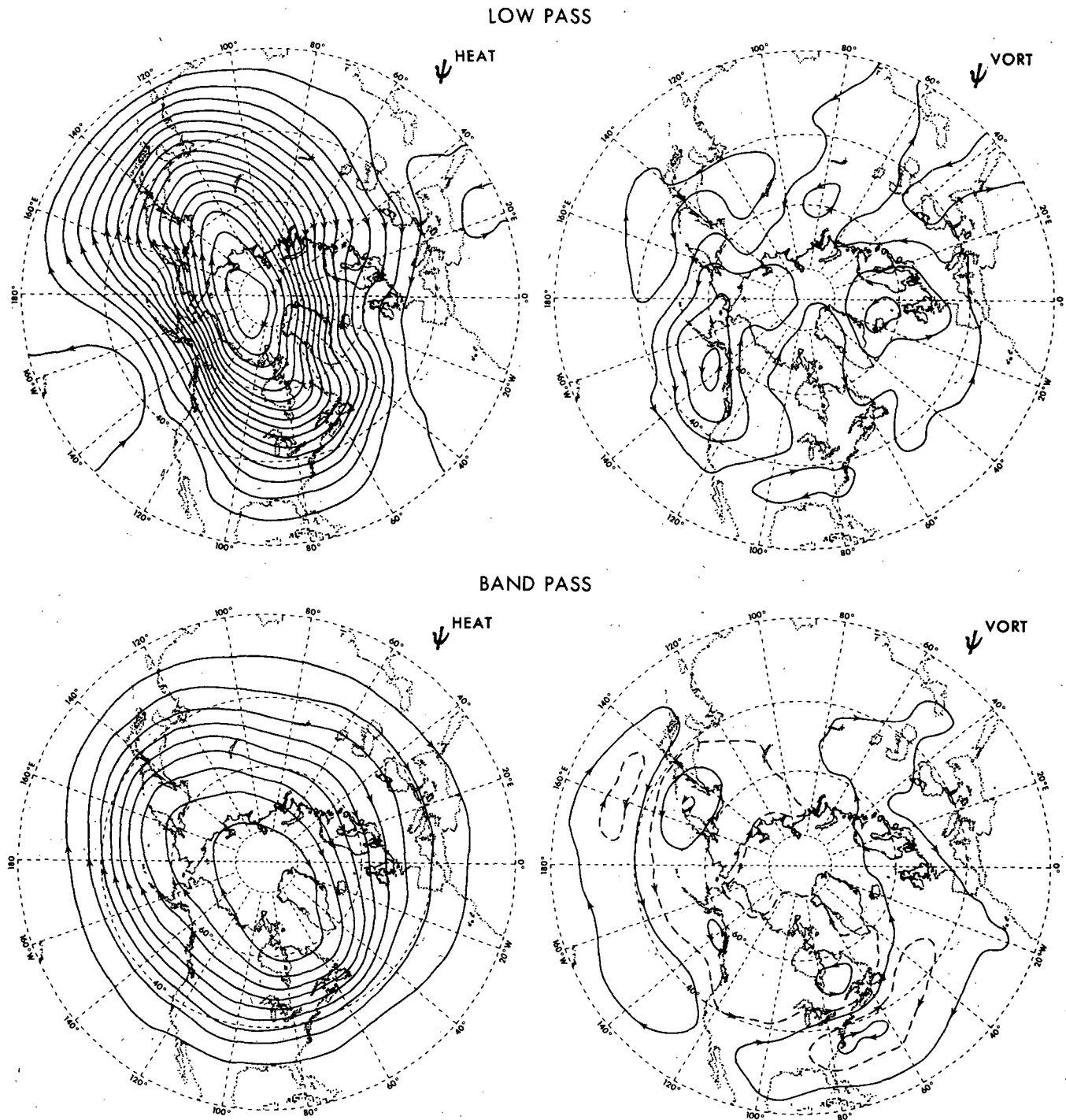


FIG. 6. Distribution of ψ^{HEAT} (left) and ψ^{VORT} (right) for winter, as determined from lowpass (upper panels) and bandpass (lower panel) filtered NMC data averaged over the atmospheric layer from 700 to 300 mb. Contour interval for solid contours in all patterns is $10 \text{ m}^2 \text{ s}^{-2}$.

(1982, Fig. 13), who showed that the transient eddies extract energy not only from the time-mean zonally-averaged flow, but also from the time-mean eddies (stationary waves). The dissipative effect of transient eddies on the stationary waves was first demonstrated

in the context of potential vorticity by Youngblut and Sasamori (1980) and Sasamori and Youngblut (1981) using data from the northern extratropics for January 1963. Our results, based upon much larger data sets, confirm their finding. Our study further

suggests that this dissipative effect arises to a large extent from the long-period large-scale transients. This finding is consistent with the analysis presented by Sasamori and Youngblut (1981), which indicates that baroclinic instability of planetary-scale eddies is enhanced in the presence of forced perturbations, and that these unstable eddies contribute significantly to the damping of the stationary waves.

While interpreting the results for D^{VORT} and D^{HEAT} (and the associated "forces" F_{ψ}^{VORT} and F_{ψ}^{HEAT}), it is important to bear in mind that we have been concerned with the strictly "interior" effects of TE fluxes. The transient eddies may also exert boundary influences on the time-mean flow. These boundary effects are realized through incorporation of TE fluxes in the top and bottom boundary conditions when an equation analogous to (6a) is solved for the three-dimensional structure of the eddy-induced tendency of the mean flow. Hence it is only after both boundary and interior effects are taken into account that we can fully investigate the net response of the atmosphere to TE forcing. However, in diagnostic budget studies of quantities such as potential enstrophy (see Section 4c) only the interior forcing terms (i.e., D^{HEAT} and D^{VORT}) need to be considered.

With regards to the implications of TE fluxes at the boundaries, we wish to draw attention to an important distinction between D^{VORT} and D^{HEAT} . The average of D^{VORT} over an entire atmospheric column is not subject to any special mathematical constraint. On the other hand, we note that

$$\int_0^{p_0} D^{\text{HEAT}} dp = f \left(\frac{\nabla \cdot \overline{\mathbf{V}'\theta'}}{\bar{S}} \right)_{p=p_0},$$

where the assumption that $\bar{S}^{-1} \nabla \cdot \overline{\mathbf{V}'\theta'} = 0$ at the top boundary has been made, and p_0 is the surface pressure. Making use of the arguments outlined by Bretherton (1966), the lower rigid boundary may conceptually be visualized as an infinitesimally thin sheet centered at the $p = p_0$ surface and situated between $p = p_0^-$ and $p = p_0^+$, where $p_0^- < p_0 < p_0^+$. Any flow with eddy heat fluxes at the lower boundary may then be formally treated as equivalent to a flow with no flux at $p = p_0^+$, but with a concentration of D^{HEAT} within the thin sheet, such that

$$\int_{p_0^-}^{p_0^+} D^{\text{HEAT}} dp = -f \left(\frac{\nabla \cdot \overline{\mathbf{V}'\theta'}}{\bar{S}} \right)_{p=p_0}.$$

It follows that

$$\int_0^{p_0^+} D^{\text{HEAT}} dp = 0,$$

$$\int_0^{p_0^+} F_{\psi}^{\text{HEAT}} dp = 0.$$

Hence the averages of D^{HEAT} and F_{ψ}^{HEAT} over the

entire atmospheric column should vanish. Since the patterns for F_{ψ}^{HEAT} averaged over the atmospheric layers from 700 to 300 mb (Fig. 4a) and from 850 to 100 mb (not shown, similar to Fig. 4a) are dominated by a westward component, the above constraint requires a compensating, mainly eastward-directed F_{ψ}^{HEAT} below 850 mb. A force with such a vertical profile acts to reduce the vertical shear (or baroclinic) component of the mean flow, but has no effect on the vertically averaged (or barotropic) component of the mean flow.

The combined effects due to TE fluxes both in the interior and at the boundaries may also be investigated using the omega equation, which provides for a diagnostic relationship between the eddy forcing and its associated ageostrophic circulation. An analytic solution for the zonally averaged meridional circulation accompanying heat transports by simple baroclinic waves has been obtained by Phillips (1954). In the middle latitudes, this eddy-induced circulation takes the form of a thermally indirect cell. The ageostrophic motion associated with this cell brings about a deceleration of the upper tropospheric flow and an acceleration of the lower tropospheric flow, so that the vertical shear of the mean flow is reduced, whereas the barotropic component remains unaltered. These analytic results are in qualitative agreement with the discussion in the preceding paragraph pertaining to the vertical distribution of F_{ψ}^{HEAT} .

Acknowledgments. We are indebted to Dr. A. H. Oort for providing us with the GFDL data set, and to Drs. I. M. Held, J. D. Mahlman and G. H. White for their constructive comments on earlier versions of this manuscript. NCL is supported at the Geophysical Fluid Dynamics Program by NOAA Grant 04-7-022-44017.

REFERENCES

- Blackmon, M. L., 1976: A climatological spectral study of the 500 mb geopotential height of the Northern Hemisphere. *J. Atmos. Sci.*, **33**, 1607-1623.
- , J. M. Wallace, N-C. Lau and S. L. Mullen, 1977: An observational study of the Northern Hemisphere wintertime circulation. *J. Atmos. Sci.*, **34**, 140-153.
- Bretherton, F. B., 1966: Critical layer instability in baroclinic flows. *Quart. J. Roy. Meteor. Soc.*, **92**, 325-334.
- Edmon, H. J., B. J. Hoskins and M. E. McIntyre, 1980: Eliassen-Palm cross sections for the troposphere. *J. Atmos. Sci.*, **37**, 2600-2616.
- Ertel, E., 1942: Ein neuer hydrodynamischer Wirbelsatz. *Meteor. Z.*, **59**, 277-281.
- Hartmann, D. H., 1977: On potential vorticity and transport in the stratosphere. *J. Atmos. Sci.*, **34**, 968-977.
- Holopainen, E. O., 1978: On the dynamic forcing of the long-term mean flow by the large-scale Reynolds's stresses in the atmosphere. *J. Atmos. Sci.*, **35**, 1956-1604.
- , 1982: Transient eddies in mid-latitudes: Observational aspects. *Large-Scale Dynamical Processes in the Atmosphere*, B. J. Hoskins and R. P. Pearce, Eds., Academic Press.

- , and A. H. Oort, 1981a: Mean surface stress curl over the oceans as determined from the vorticity budget of the atmosphere. *J. Atmos. Sci.*, **38**, 262–269.
- , and —, 1981b: On the role of large-scale transient eddies in the maintenance of the vorticity and enstrophy of the time-mean atmosphere flow. *J. Atmos. Sci.*, **38**, 270–280.
- Holton, J. R., 1974: *An Introduction to Dynamic Meteorology*. Academic Press, 319 pp.
- Lau, N.-C., 1979: The observed structure of the tropospheric stationary waves and the local balances of vorticity and heat. *J. Atmos. Sci.*, **36**, 996–1016.
- , and J. M. Wallace, 1979: On the distribution of horizontal transports by transient eddies in the northern wintertime circulation. *J. Atmos. Sci.*, **36**, 1844–1861.
- , and A. H. Oort, 1981: A comparative study of observed Northern Hemisphere circulation statistics based on GFDL and NMC analyses. Part I: The time-mean fields. *Mon. Wea. Rev.*, **109**, 1380–1403.
- , and —, 1982: A comparative study of observed Northern Hemisphere circulation statistics based on GFDL and NMC analyses. Part II: Transient eddy statistics and the energy cycle. *Mon. Wea. Rev.*, **110** (in press).
- , G. H. White and R. L. Jenne, 1981: Circulation statistics for the extratropical Northern Hemisphere based on NMC analyses. NCAR Tech. Note TN-171 + STR, 138 pp.
- NCAR, 1978: NCAR software support library, Vol. 2. NCAR Tech. Note TN/IA-105.
- Newell, R. E., J. W. Kidson, D. G. Vincent and G. J. Boer, 1974: *The General Circulation of the Tropical Atmosphere and Interactions with Extratropical Latitudes*, Vols. 1 and 2. The MIT Press, 258 and 371 pp.
- Oort, A. H., and E. M. Rasmusson, 1971: *Atmospheric Circulation Statistics*. NOAA Prof. Paper 5, U.S. Government Printing Office, Washington DC [NTIS COM-72-50295].
- Phillips, N. A., 1954: Energy transformations and meridional circulations associated with simple baroclinic waves in a two-level, quasi-geostrophic model. *Tellus*, **6**, 273–286.
- Saltzman, B., 1962: Empirical forcing functions for the large-scale mean disturbances in the atmosphere. *Geophys. Pura Appl.*, **52**, 173–188.
- Sasamori, T., and C. E. Youngblut, 1981: The nonlinear effects of transient and stationary eddies on the winter mean circulation. Part II: The stability of stationary waves. *J. Atmos. Sci.*, **18**, 87–96.
- Savijärvi, H., 1978: The interaction of the monthly mean flow and the large-scale transient eddies in two different circulation types. Part III. *Geophysica*, **15**, 1–16.
- Schubert, S. D., and G. F. Herman, 1981: Heat balance statistics derived from four-dimensional assimilations with a global circulation model. *J. Atmos. Sci.*, **38**, 1891–1905.
- Staley, D. D., 1960: Evaluation of potential vorticity changes near the tropopause and the related vertical motion, vertical advection of vorticity and transfer of radioactive debris from stratosphere to troposphere. *J. Meteor.*, **17**, 591–620.
- Tomatsu, K., 1979: Spectral energetics of the troposphere and lower stratosphere. *Advances in Geophysics*, Vol. 21, Academic Press, 289–405.
- Wiin-Nielsen, A., and J. Sela, 1971: On the transport of quasi-geostrophic potential vorticity. *Mon. Wea. Rev.*, **99**, 447–459.
- Youngblut, C., and T. Sasamori, 1980: The nonlinear effects of transient and stationary eddies on the winter mean circulation. Part I: Diagnostic analysis. *J. Atmos. Sci.*, **37**, 1944–1957.